



HAL
open science

Pelagic stocks and carbon and nitrogen uptake in a pearl farming atoll (Ahe, French Polynesia)

Martine Rodier, Christel Pinazo, Claire Seceh, David Varillon

► To cite this version:

Martine Rodier, Christel Pinazo, Claire Seceh, David Varillon. Pelagic stocks and carbon and nitrogen uptake in a pearl farming atoll (Ahe, French Polynesia). *Marine Pollution Bulletin*, 2021, 167, pp.112352. 10.1016/j.marpolbul.2021.112352 . hal-03272657

HAL Id: hal-03272657

<https://hal.science/hal-03272657>

Submitted on 24 Apr 2023

HAL is a multi-disciplinary open access archive for the deposit and dissemination of scientific research documents, whether they are published or not. The documents may come from teaching and research institutions in France or abroad, or from public or private research centers.

L'archive ouverte pluridisciplinaire **HAL**, est destinée au dépôt et à la diffusion de documents scientifiques de niveau recherche, publiés ou non, émanant des établissements d'enseignement et de recherche français ou étrangers, des laboratoires publics ou privés.



Distributed under a Creative Commons Attribution - NonCommercial 4.0 International License

PELAGIC STOCKS AND CARBON AND NITROGEN UPTAKE IN A PEARL FARMING ATOLL (AHE, FRENCH POLYNESIA)

Martine Rodier^{1,3}, C. Pinazo¹, C. Seceh¹, D. Varillon²

¹ *Institut de Recherche pour le Développement, UMR 7294 MIO (Institut de Recherche Pour le Développement, Aix Marseille Université, Centre National de la Recherche Scientifique, Université de Toulon), UM 110, 13288 Marseille, France*

² *Institut de Recherche pour le Développement, US 191 IMAGO, BP A5, 98848 Nouméa cedex, New-Caledonia*

³ *Institut de Recherche pour le Développement, UMR 241 EIO (Université de la Polynésie française, IRD, Institut Louis Malardé (ILM), Ifremer), B.P. 6570 - 98702 Faa'a, Tahiti, French Polynesia*

Corresponding author: Martine Rodier, martine.rodier@ird.fr

ABSTRACT

This study reports the first measurements of nitrogen uptake and new data on carbon fixation (¹⁵N/¹³C incorporation) for two size-fractionated phytoplankton (<2 μm and >2 μm), on organic matter, and phytoplankton stocks in Ahe lagoon. Data were collected between November and December 2017, during the hot season with prevailing trade winds. Ammonium and nitrate uptake data (7.58 to 39.81 and 1.80 to 21.43 μmol N m⁻³ h⁻¹, respectively) suggest a rapid turn-over of N-nutrients in the water column and show that primary production was largely sustained by recycled nitrogen providing 68% of the pelagic N demand. These results highlight the spatial heterogeneity of the measured processes linked to the local hydrodynamics, exhibiting higher regenerated production in the more exploited south-western part of the lagoon and a higher proportion of new production in the north. Intense nutrient recycling appears to promote nanophytoplankton production which is critical for pearl oyster growth.

Key words: Nitrogen uptake, primary production, phytoplankton composition, atoll lagoon, pearl farming, French Polynesia

1. Introduction

Atoll lagoons are generally highly productive ecosystems compared to the surrounding oligotrophic ocean (Hatcher, 1997). They support fisheries and aquaculture production that can make significant contributions to the economic development of many Pacific island countries. There are 84 atolls in French Polynesia, 77 of which belong to the Tuamotu Archipelago, a highly productive black pearl oyster (*Pinctada margaritifera*) farming site. Black pearl production currently ranks second only to tourism among the sources of income in French Polynesia. However, over the two past decades, this sector has declined and many farms had to close with major consequences for the local population. This decline has several reasons, including high stocking densities of pearl oysters potentially coupled with environmental changes causing algal blooms and massive mortalities as well as poor management of regional and international trade (Andréfouët et al., 2012). In this context, several research programs were launched to learn more about the biological processes related to pearl oyster farming and possible interactions with the environment (Andréfouët et al., 2012; Gueguen et al., 2016). These programs were to provide appropriate management recommendations and develop models and new tools specifically designed to achieve a sustainable use of atoll resources.

Atoll lagoons are isolated marine ecosystems and their remoteness and poor accessibility often make it difficult to carry out field studies. Modelling can therefore be a cost-effective way to help understand the often complex ecosystem dynamics and assess the importance of the various physico-biogeochemical processes, particularly with regard to the oyster food web (Duarte et al., 2003; Webster and Harris, 2004). In the past decade, several numerical models have been developed and implemented for the Ahe atoll (Tuamotu Archipelago) which hosts an important pearl oyster farming industry. One of those models is a 3D biophysical model based on the MARS3D hydrodynamic model (Dumas et al., 2012), which was extended by adding a larval transport model (Thomas et al. 2014). In parallel, a Dynamic Energy Budget (DEB) model of the larval stage was developed considering the eco-physiology of *P. margaritifera* (Fournier et al. 2012, Sangare et al. 2020; Thomas et al., 2011) and coupled with the 3D physical model (Thomas et al. 2016). The coupling of such a DEB model with a physico-biogeochemical model that can simulate the variability of food sources (plankton) in time and space represents a significant advancement compared to the traditional approach using temporal and spatial interpolations of sparse *in situ* measurements.

The success of black pearl aquaculture strongly depends on environmental parameters and pelagic food sources that can affect larval development and settlement as well as adult development

and reproduction of *P. margaritifera*. While this species is benthic in the wild, when farmed, it is suspended on vertical lines in water-column and is therefore highly dependent on the availability of plankton for feeding (Fournier et al., 2012a; Pouvreau et al., 2000; Thomas et al., 2016). Thus, while pearl oyster farms negatively affect phytoplankton abundance and primary production through grazing, they may increase production by supplying the water column with nutrients (Lacoste and Gaertner-Mazouni, 2016). The development of a new biogeochemical model should therefore consider the pelagic food web and be able to account for the effects of oysters on lower trophic levels such as phytoplankton. This model is currently in its first phase of development for the Ahe lagoon (ECO3M-Atoll model configuration) and uses the environmental and planktonic data collected over 10 years to constrain the model parameters. This dataset includes chlorophyll a (Chla), phytoplankton size structure and composition (Charpy et al., 2012; Thomas et al., 2010), prokaryotic diversity and dynamics (Bouvy et al., 2012; Michotey et al., 2012), zooplankton biomass and composition, grazing by oysters (Fournier et al., 2012a; Pagano et al., 2012; 2017), primary production and photosynthetic parameters (Lefebvre et al., 2012), as well as nutrient fluxes at the sediment-water interface or produced in the water column by the cultured pearl oysters and their associated epibionts and biofouling (Lacoste and Gaertner-Mazouni, 2016, and references herein). However, several characteristics of the Ahe lagoon remain less well documented such as the taxonomic composition of nano- and microphytoplankton (Dupuy et al., 2009; Fournier et al., 2012a) and the C, N and P content of organic matter. Finally, no information exists on the *in situ* N uptake by phytoplankton at Ahe and at the entire Tuamotu Archipelago, with the exception of some preliminary data on N₂ fixation (Charpy-Roubaud and Charpy, 2001). The only information on nitrogen utilization by phytoplankton in Tuamotu atoll lagoons was collected in bioassay experiments to investigate nutrient limitation (Dufour et al., 1999; Ferrier-Pagès and Furla, 2001; Sakka et al., 1999), although without discriminating between the different chemical forms of nitrogen.

In November and December 2017, a field campaign was conducted in Ahe lagoon as part of the MANA (MANagement of Atoll) project. The main objectives included the provision of new insights into the ecosystem dynamics and functioning in Ahe lagoon by acquiring new and innovative pelagic data to calibrate a new ecosystem model. Measurements included hydrological parameters, particulate and dissolved matter (C, N, P), chlorophyll, nano- and microphytoplankton taxonomy, and phytoplankton C and N uptake. For the first time, *in situ* data on nitrogen uptake for two phytoplankton size fractions (<2 µm and >2 µm) could be collected and combined with carbon fixation and other environmental and phytoplankton data. Here, we used the dual ¹⁵N/¹³C isotopic method to measure nitrate, ammonium, and carbon uptake rates and estimate the amount of

production that is sustained by new and regenerated nitrogen. In addition to the usual nutrient measurements, these nitrogen uptake data are essential to determine the effective trophic status of the lagoon and to better understand the nitrogen cycling and the ability of planktonic food-webs to sustain intense pearl farming. More generally, these data are useful to improve our understanding of lagoon ecosystem functioning and ecosystem-level effects of pearl farming, and to develop realistic biophysical models as set out in the MANA project.

2. Material and methods

2.1 Study site

The Ahe atoll is located in the northwestern part of the Tuamotu Archipelago (French Polynesia), in the South Pacific Ocean (14°29'S, 146°18'W). The lagoon is of medium size (145 km²) and deep with a maximum depth of 71 m and an average depth of 41 m (Andréfouët et al., 2020). It is semi-closed with a pass located on the northwestern side and few reef flats spillways (“*hoa*”) mostly in the southern and northwestern parts of the rim (Fig. 1). The lagoon is weakly flushed with a renewal time of 252 days and an average e-flushing time of about 80 days (Dumas et al., 2012). The lagoon is largely covered by pearl farming concessions which are distributed along its border (Supplementary Fig. S1), especially in the southwestern part (referred after as SW lagoon), which concentrates the highest populations of cultured and wild oysters (Andréfouët et al., 2016). In contrast, there is no farming activity in the deeper central area and little in the northeast of the lagoon. There is no weather station on the atoll and the meteorological data are available from Takaroa station (Météo-France) located 100 km east of Ahe.

2.2 Water sampling and CTD profiler

Samples were collected from November 27 to December 7, 2017 at the beginning of the hot season during a period of moderate trade winds, and in weak La Niña conditions according to the Oceanic Niño Index (https://origin.cpc.ncep.noaa.gov/products/analysis_monitoring/ensostuff/ONI_v5.php). Field operations were conducted with a small boat from a field laboratory located near the main village. All sampling was done between 7:00 and 12:00 AM, mainly at rising tide.

Five main stations in the lagoon (L0, L1, L4, L8, L10; Fig. 1) were sampled for environmental, phytoplankton stock and C and N uptake measurements, with three daily samplings at each station, except L0 which was sampled only twice. These stations corresponded to some of the historical stations sampled since 2008 and were selected to represent different pearl farming (Supplementary

Fig. S1) and hydrodynamic conditions according to Dumas et al. (2012). Station L1 was shallower (24 m deep) than the other stations (up to 36 m) and was located in the SW lagoon, in an intensive oyster farming area with many long lines of 200m supporting reared oysters and spat collectors. Station L0 was also located in the SW lagoon but near the village and outside the long-lines area. Stations L8 and L10 were located close to the atoll rim in the eastern and northwestern part of the lagoon, respectively, with moderate farming activity. Finally, the station L4 was near the pass and outside the rearing concessions. At each station, a CTD profiler (SBE 19+, SeaBird) was deployed from the sub-surface down to the bottom, recording vertical profiles of temperature, salinity, fluorescence and PAR (Photosynthetic Available Radiation). Fluorescence was calibrated with measured chlorophyll a (Chla). Water samples for nutrients, organic matter, phytoplankton and C and N uptake measurements were collected from two depths (3 m and 20-30 m) using a 5-litre Niskin bottle. In this paper, data are presented as depth-averaged values over the different sampling days, given the absence of short-term meteorological events during the study period.

Additional CTD, nutrients and Chla data (without organic matter and C and N uptake measurements) were collected once in the northeast of the lagoon (L11, L12) at 3 and 30 m.

Finally, a transect dedicated to surface Chla and phytoplankton taxonomy measurements with CTD profiles at each station was done twice on November 28 and December 2 from the SW lagoon (T1 to T5) to the central area (T6 to T11) and finally near and in the pass (T12-T13). Note that T1 is located at the northeast limit of the “green lagoon” (as it is called by the local population), which is a particular environment isolated from the main lagoon by a submerged reef (Fig. 1).

2.3 Inorganic nutrients and dissolved organic matter (C, N, P)

Nitrate and nitrite (NO_x) and phosphate (PO_4^-) samples were HgCl_2 -poisoned and analyzed after the cruise by colorimetric methods using a segmented-flow Auto-Analyzer (AA3, SEAL corporation, Mequon, WI, USA), as described in Raimbault et al. (1990) and Aminot and K  rouel (2007). Ammonium (NH_4^+) samples were immediately analyzed by fluorometry using a Turner Trilogy fluorometer (module No 7200-041) according to the Holmes et al. (1999)’s method. DIN refers here to $\text{NO}_x + \text{NH}_4^+$. The detection limits for NO_x , PO_4^- and NH_4^+ were 0.05, 0.02 $\mu\text{mol L}^{-1}$ and 0.01 $\mu\text{mol L}^{-1}$ respectively.

Samples for dissolved organic matter (DOM) measurements were taken directly, without pre-filtration, from the Niskin bottle into 25 mL Schott bottles (precombusted at 450  C, overnight), immediately acidified with 50 μL of H_2SO_4 (4.9N) and then stored until analyses. Organic matter was digested by persulfate wet-oxidation technique and converted to inorganic end products, which were

then measured by colorimetry and Auto-Analyzer as described in Raimbault et al. (1999). Total organic N and P were first calculated as total inorganic nitrogen and phosphorus measured after wet oxidation minus inorganic nitrogen ($\text{NO}_x + \text{NH}_4^+$) or phosphate (PO_4^-) measured separately at the same sampling depth, as described above. Dissolved organic matter (DOC, DON and DOP) was then calculated as total organic matter minus particulate organic C and N (POC, PON) obtained by mass spectrometer (cf. & 2.5) and particulate organic P (POP) estimated from PON concentrations using Redfield ratio.

2.4 *Phytoplankton analysis*

Chlorophyll: *In situ* chlorophyll a (Chla) concentrations were measured fluorometrically after methanol extraction (Le Bouteiller et al., 1992), using a Turner Design fluorometer equipped with the module No 7200-040 (Chl-a extracted-acidification). Total Chla concentrations were determined from 0.25 L water samples filtered onto GF/F Whatman filters. In parallel, 0.50 L water samples were filtered separately onto 2 μm and 10 μm Nucleopore filters for the $>2\mu\text{m}$ and $> 10\mu\text{m}$ Chla size class. The 10 μm size-fractionation was performed only once at the main stations. Chla $<2 \mu\text{m}$ (Total Chla minus Chla $>2 \mu\text{m}$) and Chla $>2 \mu\text{m}$ represent pico- and nano-microphytoplankton proxies, respectively.

Microscopic analyses: 1.5 L samples were collected from the Niskin bottle and fixed with a borate-buffered formalin solution (4-5 % v:v final concentration). Phytoplankton was then concentrated ~ 10 times by sedimentation and siphoning of the overlying seawater after 48h. Counting and identification of phytoplankton were carried out with a Wild M40 inverted microscope with phase contrast, according to the Utermöhl technique. The sedimented volume was 50 mL or less, depending on the density of the organisms and the presence of detritus. Identification was done to the lowest possible taxa using appropriate keys (Tomas, 1996; WoRMS, 2019). Tiny organisms could not be adequately classified by inverted microscope method and were grouped in the unidentified 3-4 μm phytoplankton category (3-4 μm phytoP).

2.5 *Carbon and nitrogen uptake and organic particulate matter*

Photosynthetic carbon fixation (primary production, P) and ammonium and nitrate uptake rates (ρNH_4^+ , ρNO_3^-) were measured three (two at L0) times at the L stations at 3 and 20-30 m, using the dual $^{13}\text{C}/^{15}\text{N}$ isotopic method as described in detail in Raimbault et al. (2008 and references herein). At each depth, water samples were collected in duplicate into acid-leached 1.2 L polycarbonate bottles. All bottles were enriched with 1 mL of a $\text{NaH}^{13}\text{CO}_3$ solution (24 g L^{-1} , 99.2 % ^{13}C , EURISOTOP) for C fixation and half with 200 μL of $^{15}\text{NH}_4\text{Cl}$ or K^{15}NO_3 solution (0.5 mmol N L^{-1} ,

98-99% ^{15}N), allowing simultaneous measurements of NH_4^+ and NO_3^- uptake at each depth. Immediately after adding the tracers, the bottles were incubated *in situ* at their respective sampling depths. Incubations started around 13:00 and lasted between 4 and 5 hours. At the end of incubation, 0.6 L from each bottle was filtered directly onto 25 mm Whatmann GF/F pre-combusted glass fiber (total uptake) and 0.6 L was fractionated by serial filtration through 2 μm polycarbonate Millipore and GF/F filters (uptake by the $<2 \mu\text{m}$ fraction). At the five main stations, an additional bottle was collected at 3 m, enriched with ^{13}C and ^{15}N and immediately filtered to determine the isotopic background ($t=0$ enrichment). All filters were then dried for 24 h and stored until mass spectrometry analysis within 2 months. The dual isotopic enrichment and particulate organic carbon and nitrogen (POC, PON) analyses were performed using an Integra-CN mass spectrometer, calibrated with glycine reference and regularly controlled using reference materials from the International Atomic Energy Agency (IAEA, Analytical quality control services). Before analysis, the filters were acidified with 100 μL H_2SO_4 (0.5N) to remove inorganic matter. Carbon fixation rates were calculated with a measured $t=0$ value of $1.093 \pm 0.004 \%$ and NO_3^- and NH_4^+ uptake rates with a $t=0$ value of $0.367 \pm 0.003 \%$.

2.6 Statistical analysis

Paired *t*-tests were applied to test differences between the two Chl a size fractions, between 20-30 m-depth and 3 m-depth values of different parameters and between NH_4^+ and NO_3^- uptake rates. One-way ANOVA method was used to test the differences between stations for different parameters and post-hoc tests were conducted to identify outliers and homogeneous groups. Before analysis, all data were log-transformed [$\log(x + 1)$]. In each case, we checked that the residuals were normally distributed, using Shapiro Wilks Test. All statistical tests were performed using Statistica 7 Software.

3. Results

3.1 Environmental background

During the study period, the trade winds were constant and moderate (5.4 m s^{-1} on average) and rainfall was almost nil, except on Day 5 when it rained a little during the night. The lagoon remained unstratified during the whole period with quite homogeneous temperature and salinity profiles and values ranging from 27.8 to 29.5 $^{\circ}\text{C}$ (28.4 $^{\circ}\text{C}$ on average) and 35.98 to 36.46 (36.25 on average), respectively (Fig. 2). At the lagoon scale, the temperature and salinity distribution revealed a spatial heterogeneity with higher surface temperatures and salinities in the SW area and lower values in the northeastern part. Low temperature and salinity were also measured in front of the pass.

The lagoon was low N- and P-nutrients (Table 1), except in the northeast (Stations L11, L12) where slightly higher nitrate concentrations were recorded. In comparison, mean dissolved organic matter (DOM) concentrations ranged between 74.4 and 85.6 $\mu\text{mol L}^{-1}$ for DOC, between 9.0 and 12.2 $\mu\text{mol L}^{-1}$ for DON and between 0.4 and 0.5 $\mu\text{mol L}^{-1}$ for DOP (Table 1), with no clear spatial pattern (ANOVA, $P > 0.1$ for C, N, and P). DON concentrations were about 26 times higher than DIN concentrations and accounted for most of the nitrogen in the water column (>95%), while the difference was less pronounced for P with less than 1.5 times more DOP than PO_4^- . As a result, the DIN: PO_4^- ratios (< 2) were much lower than the DON:DOP ratios (~ 22). The particulate organic matter (POM) pool (collected on GF/F filters) was smaller than DOM pool with mean values between 8.24 and 17.72 $\mu\text{mol L}^{-1}$ for POC and between 1.06 and 1.93 $\mu\text{mol L}^{-1}$ for PON.

3.2 Phytoplankton biomass, size structure and taxonomic composition of the >2 μm assemblages

Total Chla concentrations ranged from 0.13 to 0.38 mg m^{-3} with an average of $0.20 \pm 0.14 \text{ mg m}^{-3}$ at the L stations (Table 1) but reached 0.63 mg m^{-3} at T1 in surface (Fig.2). Concentrations were significantly higher in the SW lagoon than in the rest of the lagoon (ANOVA, $P < 0.01$). There was no statistical difference between Chla measured at 3 m and at 20-30 m (paired t -test, $P > 0.1$). Similarly, *in situ* fluorescence profiles were fairly homogenous down to 20-30 m with a slight increase below or near the bottom (Fig. 2). Chlorophyll biomass (B_{Chla}) was dominated by the picophytoplankton with a contribution of the $< 2 \mu\text{m}$ fraction ranging from 63 to 89 % of ($79 \pm 7 \%$). The percent contribution of $> 2 \mu\text{m}$ fraction to the total B_{Chla} was higher in the SW lagoon, but the spatial difference was not significant (paired t -test, $P > 0.1$). It should be noted that 68% of $B_{\text{Chla}} > 2 \mu\text{m}$ was less than 10 μm , with a maximum of 88% at L1.

Microscopic analysis of samples taken at 3 m along the transect (Fig. 3) showed a decrease of three orders of magnitude in nano-microphytoplankton abundance from T1 to T11 ($4.4 \cdot 10^6$ at T1 to $8.9 \cdot 10^3 \text{ cell L}^{-1}$ at T11) and revealed changes in the taxonomic composition of the assemblages. Overall, the assemblages were largely dominated by dinoflagellates and prymnesiophytes (mainly *Gephyrocapsa*, *Syracosphaera*) which were abundant at all stations. Four genera dominated the dinoflagellate assemblages: *Heterocapsa*, *Gymnodinium*, *Triplos* and *Prorocentrum*, in decreasing order of abundance. Prasinophytes (mainly *Pyramimonas*) and unidentified nanophytoplankton composed of 3-4 μm spherical unicellular organisms (referred to here as 3-4 μm nanoP) were predominant in the SW lagoon, and almost disappeared outside this area. In contrast, diatoms (mainly *Nitzschia spp*) were rare in the south and their abundance increased elsewhere while remaining relatively low. Cyanobacteria were observed along the transect, except in the “green lagoon” (T1).

This group was dominated by the unicellular-colonial cyanobacterium *Merismopedia* at the shallowest stations (T3, T5) and by two filamentous cyanobacteria *Spirulina* and *Trichodesmium* at the other stations.

3.3 Metabolic processes: primary production and nitrogen uptake

Primary production (P) showed a clear spatial distribution, with mean values ~ 3 times higher in the SW region (2.04 to 2.40 mg C m⁻³ h⁻¹) than in the rest of the lagoon (0.60 to 0.86 mg C m⁻³ h⁻¹) (Fig. 4; Table 2). While primary production was dominated by picophytoplankton, the primary production of the >2 μm fraction represented 25 ± 12 % of total P on average and reached 33 to 48 % at 3 m at L1 and L4. The biomass-specific primary production rates (P/B_{Chla}) of the >2 μm fraction were significantly higher than the P/B_{Chla} of the <2 μm fraction (Table 2; paired *t*-test; *P* < 0.05), with mean values ranging from 4.59 to 13.23 mg C mg Chla⁻¹ h⁻¹ and from 3.44 to 6.23 mg C mg Chla⁻¹ h⁻¹, respectively. The highest P/B_{Chla} values were obtained at L1 and the lowest at L10, regardless of the size fraction (Fig. 5), but the spatial difference could not be demonstrated statistically.

Mean ammonium uptake rates (ρNH₄⁺) ranged from 7.58 to 39.81 μmol N m⁻³ h⁻¹ and had a contrasting spatial distribution (Table 2, Fig. 6) with significantly higher rates in the SW lagoon (ANOVA, *P* < 0.005). NH₄⁺ uptake of the > 2μm fraction represented less than 30 % of total uptake, except at L1 where it reached 57% on average. Nitrate uptake rates (ρNO₃⁻) were lower than NH₄⁺ uptake rates at all stations (paired *t*-test; *P* < 0.05), with mean values varying from 1.80 to 21.43 μmol N m⁻³ h⁻¹. Stations L0 and L4 differed from the other stations by significantly higher and lower NO₃⁻ uptake rates, respectively (ANOVA, *P* < 0.05). The >2 μm fraction contributed ~ 37 % of the total NO₃⁻ uptake in the SW area and over 50 % in the other sites with a maximum at L10 (73 %), which differs from the NH₄⁺ uptake pattern. Noticeably, the P/ρNH₄⁺ ratios were lower than 6.4, except at 3m at L4 where it reached 9.5, while P/ρNO₃⁻ ratios were > 9 with higher values at L1 and L4 (>20).

The *f*-ratio, which is the ratio of NO₃⁻ uptake to the summed uptake of NO₃⁻ and NH₄⁺ (Harrison et al., 1987) was used to estimate the proportion of new and regenerated production to total production (Table 2), an *f*-ratio < 0.5 indicating a dominance of regenerated production. The *f*-ratios were significantly lower at L1 and L4 than at the other stations (*P* < 0.005) and the higher values were mainly due to the fraction >2 μm.

4. Discussion

In the first part of this discussion, we will compare our data with previously published data from Ahe lagoon in order to provide a more general context. In the second part, we will focus on the new data on N-uptake and new and regenerated production.

4.1 Comparison of our campaign with previous studies: environmental context and primary production

Our field campaign in November and December 2017 coincided with the hot season (temperatures typically increase from October onward) and ended before the start of the rainy season. The trade wind regime that prevailed during the 11 sampling days of our study is the most frequent weather regime in the region (Dutheil et al., 2020). The lack of short-term events during our sampling period (winds fairly constant and almost no rain) created relatively stable conditions which we assume to be representative of hot, dry, and trade wind conditions in the area. As a result, the water-column was fairly homogeneous with only a very weak thermo-haline stratification (Fig. 2), which appears to be a typical situation for this lagoon (present in 80% of observations in 2008-2009), due to both wind direction/intensity and deep overturning circulation (Dumas et al., 2012). *In vivo* fluorescence and Chla were homogeneously distributed with depth due to vertical mixing as observed in Charpy et al. (2012) and could thus represent a common pattern in the lagoon, although this needs further confirmation. The prevailing trade winds and the associated circulation pattern may also explain the lagoon-wide temperature gradient observed in this study, with cooler bottom waters upwelled windward on the eastern side of the lagoon and warm surface waters pushed downwind toward the SW area as described in Dumas et al. (2012). Finally, under trade winds the lagoon is partitioned into three circulation cells that trap water and structure the e-flushing times: a narrow and shallow southern cell (stations L0 and L1), a deep and large northern cell (Stations L8, L10, L11, and L12), both with long e-flushing times of around 80-100 days, and a central cell in front of the pass (station L4) with shorter e-flushing time of 50-60 days. As postulated in previous studies on the Tuamotu atolls, the hydrodynamic regime (water exchanges and wind-driven circulation) and associated water renewal times are the main factors controlling the biogeochemical functioning of the lagoons and associated plankton dynamics (Andréfouët et al., 2001; Charpy et al., 1997; Torreton et al., 2002).

In our study, the nutrient status of the lagoon was characterized by low concentrations of readily bioavailable nutrients and potentially N-limited (sub-Redfield DIN/PO₄⁻), as observed previously in Ahe (Charpy et al., 2012; Pagano et al., 2017). The northeast corner of the lagoon (Stations L12 and L11, Table 1) presented higher nitrate concentrations which may be the signature of the local and transient internal upwelling generated by the trade winds (Fournier et al., 2012b). In comparison, dissolved organic matter concentrations were high and rich in N with DON:DOP ratios above Redfield. While data on DOM in Ahe lagoon are scarce, our mean DOC concentrations (81 μmol L⁻¹) were comparable to those recorded in August 2009 (Bouvy et al., 2012). Our DOC values were within the mid-range of those measured in other Tuamotu lagoons (Pages et al., 1997), while our mean DON

values ($10 \mu\text{mol L}^{-1}$) were in the upper range (Torréton et al., 2000). In this semi-closed lagoon, local sources of organic matter are important and multiple: coral and mucus/exudates from fixed benthic algae (Bythell and Wild, 2011), phyto- and zooplankton excretion, sloppy feeding, viral lysis (Bouvy et al., 2012; Charpy-Roubaud et al., 1990; Torréton et al., 2002), and possibly (and to a lesser extent) run-off from land. Pearl farming also represents an allochthonous organic matter source (Lacoste et al., 2014; Pouvreau, 1999). Note also that our POM values were comparable to those measured in 2008-2009 ($13.25 \mu\text{mol C L}^{-1}$ and $1.64 \mu\text{mol N L}^{-1}$; Charpy et al., 2012). Based on our mean values, the DOM pool in Ahe appeared to be 7 to 10 times higher than the POM pool and could provide at least 6 times more N than the DIN stock, even if we assume that only a low 12% of organic matter is bioavailable (lowest percentage in the review by Bronk et al., 2007).

Despite this being a low-nutrient environment, both the phytoplankton biomass (B_{Chla}) and primary production (P) remained relatively high. The large chlorophyll dataset that was collected in Ahe since 2007 contains values ranging from 0.02 to 1.19 mg m^{-3} (mean of $0.27 \pm 0.15 \text{ mg m}^{-3}$, $n = 1168$) with no obvious temporal trends over the past 10 years (Andréfouët, 2013; Charpy et al., 2012; Lefebvre et al., 2012; Pagano et al., 2017; Thomas et al., 2010; this study). There are less data on primary production available for Ahe. They were collected during four seasons, in May and October 2008 and in February and August 2009, and at four different sites along a southwest/northeast transect (Lefebvre et al., 2012). The reported P values ranged from 1.7 to $5.8 \text{ mg C m}^{-3} \text{ h}^{-1}$ (mean of $3.0 \text{ mg C m}^{-3} \text{ h}^{-1}$) in the upper 20 m of the water column with a mean phytoplankton biomass of 0.35 mg m^{-3} , which are within the upper range of measurements at other Tuamotu lagoons (Charpy et al., 1997; Torréton et al., 2002). Our mean chlorophyll concentrations ($0.22 \pm 0.14 \text{ mg m}^{-3}$) and P estimates ($1.3 \pm 0.8 \text{ mg C m}^{-3} \text{ h}^{-1}$) are in the lower range of the previously published data in Ahe, possibly due to the choice of our sampling stations and seasonal variability. Seasonal variability has been reported both for *in situ* chlorophyll and primary production with maximum/minimum ratios ranging from 1.4 to 2.1 and 1.8 to 2.1, respectively, including some differences between the $<2 \mu\text{m}$ and $>2 \mu\text{m}$ size fractions (Charpy et al., 2012; Lefebvre et al., 2012; Thomas et al., 2010). These seasonal changes were primarily attributed to changes in temperature and/or wind and nutrient availability (Lefebvre et al., 2012).

In our study, phytoplankton biomass and primary production were largely dominated by picophytoplankton, except in the SW area containing high-density oyster lines (station L1). There, primary production by the $>2 \mu\text{m}$ size fraction represented more than a third of the total P (Table 2). A similar result was reported in the study carried out in 2008-2009 (Lefebvre et al., 2012). In this highly exploited SW area of the lagoon, nanophytoplankton (with heterotrophic nanoflagellates, not

considered here) are subjected to high grazing pressure by pearl oysters (Dupuy et al., 2009; Fournier et al., 2012a) and associated filter-feeders accumulated on the culture lines (e.g., bivalves, sponges, ascidians). The organisms appear to have adapted to this high level of predation by locally increasing their P/B_{Chla} ratio (Fig. 5) which allows them to remain relatively abundant and productive. Such an adaptive strategy has already been described before (Lefebvre et al., 2012) which suggests that this strategy may have been operating successfully for some years due to the high aquaculture pressure, and shows some stability in ecosystem functioning of the SW lagoon. Our results also showed that nanophytoplankton outperformed picophytoplankton in terms of ammonium uptake in this SW part of the lagoon (see below) which affords them a growth advantage. A highly productive nanophytoplankton compartment is essential for pearl oyster farming as it represents a large portion (90%) of the oyster diet and a direct source of C (and N) for juveniles and adults (Dupuy et al., 2009; Fournier et al., 2012a; Loret et al., 2000).

4.2 Nitrogen uptake, new versus regenerated production: a new dataset

The present study provided the very first estimates of N uptake rates by phytoplankton in Ahe lagoon and allowed to assess the part of new and regenerated production. It should be kept in mind, however, that our estimates are based on simple measurements of NO_3^- and NH_4^+ uptake. This assumes in particular that regenerated production relies exclusively on NH_4^+ uptake which may result in some underestimations given that phytoplankton can also use DON components (Bronk et al., 2007), which may be relevant considering that the lagoon is DOM-rich. At the same time, NO_3^- uptake rates only represent an accurate estimate of the amount of new production if we can assume that there is no pelagic N_2 fixation. In our study we could not assess the importance of pelagic N_2 fixation as there is no information available for Ahe and only one dataset for the Tuamotu lagoons (Charpy-Roubaud et al., 2001 for the Tikehau atoll). In addition, it is difficult to distinguish between allochthonous (“new”) NO_3^- inputs and NO_3^- regenerated from organic matter. We also cannot exclude the possibility of having overestimated phytoplankton NH_4^+ uptake due to heterotrophic uptake, given that the measured $P/\rho NH_4^+$ ratios were lower than the Redfield ratio (Raimbault and Garcia, 2008).

With this being said, the N uptake data presented here provided good indications of phytoplankton N demand in Ahe lagoon. They revealed that active N uptake by phytoplankton was much higher in the lagoon than in the surrounding ocean (Raimbault and Garcia, 2008) and suggested a rapid turnover of N-nutrients, which could be sufficient to explain the low ambient DIN pools. Our results also showed that a large part of the primary production of the lagoon was sustained by regeneration processes. This was highlighted by the 1.3 to 4.2 times higher NH_4^+ uptake rates at all

stations compared to NO_3^- uptake. We found that recycled nitrogen could sustain 68% (52% to 80%) of N phytoplankton demand. The specific geomorphology of the atoll (deep and semi-enclosed) in combination with a long water renewal time (252 days) and intensive pearl farming may be the underlying cause for the intense and fast recycling in the lagoon, which may in turn explain the high portion of regenerated production and the higher biomass and overall production at Ahe compared to other lagoons. The production and subsequent release of high concentrations of dissolved organic matter into the water column could also contribute to the regeneration processes. The low intra-lagoon and vertical variability in DOM concentrations that were observed here and in previous studies (Bouvy et al., 2012) can only be explained by a fast turnover of the labile DOM through efficient recycling. In such a N-limited environment, it is likely that DON represents a dynamic source of bioavailable N for phytoplankton, either after regeneration via bacteria-bacterioplanktonic grazer coupling, through detritivores or filter-feeders (Bouvy et al., 2012; Rix et al., 2016; Torr ton et al., 2002), or by direct autotrophic assimilation of low molecular weight forms (Bronk et al. 2007; Ferrier-Pag s et al., 2000). More work is needed to fully understand the role of DON in regenerated production and in the nitrogen cycle. Such work could employ isotopic approaches to obtain a better quantification of and discrimination between DON autotrophic and heterotrophic use and release and between the different origins of the organic matter. The importance of mixotrophy by the nanoflagellate population should also be quantified to determine their contribution to the net community production (Ward and Follows, 2016).

Apart from illustrating the general biogeochemical functioning of the lagoon, our results also showed that the lagoon had spatially heterogeneous C and N uptake rates. A clear spatial pattern of primary production in Ahe was also reported by Lefebvre et al. (2012) for different seasons. We will therefore discuss the observed C and N uptake data for each sub-area and associated stations.

The SW area (Stations L1 and L0) clearly exhibited the highest levels of nutrient regeneration with NH_4^+ uptake rates about 3 to 4 times higher than elsewhere in the lagoon. Intense recycling appeared to stimulate phytoplankton growth and production (Fig. 4). The regeneration processes in this SW area were certainly intensified by i) a relatively shallow depth combined with a long e-flushing time and high temperatures, ii) its proximity to the atoll rim as a source of mucus-derived DOM in combination with the narrow shape of the lagoon (Bouvy et al., 2012), iii) the high-density pearl farming (Lacoste et al., 2014; Lacoste and Gaertner-Mazouni, 2016), and iv) the adjacent village and a higher population density. Regarding this last point and given the high NH_4^+ and NO_3^- uptake rates observed at the station nearest to the village (L0), the organisms there seem to have adapted to use both ammonium and nitrate. We suspect that phytoplankton near the village receive nitrate pulses

from anthropogenic effluents, groundwater lenses, and from the sediment-water interface although these still need to be quantified. With regard to identifying the source of regenerated products supporting the high NH_4^+ uptake rates at L0, it will be difficult to discriminate between the part associated with the general conditions of high recycling in the south cell and that directly linked to the area's proximity to the village and land.

Station L1 has been repeatedly sampled in the past, yielding a relative wealth of available data on the pelagic and benthic compartments which we can use for direct comparisons with our N uptake data. Based on zooplankton biomass data collected at L1 (Pagano et al., 2012) and using Ikeda's equation (Ikeda, 1985), we estimate that zooplankton excretion ($20 \mu\text{mol NH}_4^+ \text{ m}^{-3} \text{ h}^{-1}$ on average, with 88% due to heterotrophic nanoflagellates and ciliates) could support around 59 % of the NH_4^+ uptake measured at this station. The importance of bacteria as a direct source of NH_4^+ is more difficult to assess (Goldman et al., 1987). Here, we assume that bacterial populations are heavily grazed upon by protists (Bouvy et al., 2012) and that their role as a direct source of NH_4^+ (and of labile organic components from dead bacterial cells) is likely reduced, which remains to be confirmed. Excretion by fish and macro-invertebrates represents another source of ammonium at L1, especially due to the proximity to the reef and high local densities of pearl oysters. Lacoste and Gaertner-Mazouni (2016) showed that the rates of direct DIN release into the water column by suspended oysters and associated filter-feeders varied between 27.1 and $61.4 \mu\text{mol N m}^{-2} \text{ h}^{-1}$. These rates represent between 4 to 9 % of our mean NH_4^+ uptake rates which could confirm the direct contribution of pearl oyster cultures to regenerated primary production and supports the idea of a positive feedback loop between pearl oyster cultures and phytoplankton. The production of biodeposits that are easily biodegradable (feces and pseudofeces) by bivalves is also thought to increase remineralisation processes, although in the case of *P. margaritifera* the feces are largely composed of mineral matter (Pouvreau et al., 2000). Finally, we measured average benthic NH_4^+ fluxes of $5 \mu\text{mol h}^{-1} \text{ m}^{-2}$ at L1 (unpublished data), i.e., less than 2% of the phytoplankton NH_4^+ demand. Although low, this is consistent with previous estimates (Gaertner-Mazouni et al., 2012; Lacoste and Gaertner-Mazouni, 2016). High regeneration in the pelagic compartment with intensification of the cycling within the microbial loop may cause a disconnect of the surface production from the sediment and benthic micro- and macrofauna (Bronk et al., 2007) which does indeed seem to be the case in the SW part of the lagoon. These results suggest that most of the nutrient recycling that fuels the pelagic compartment takes place in the water column, particularly in this area. In contrast to other stations where NH_4^+ uptake is typically dominated by picoplankton and NO_3^- uptake by nanophytoplankton (Glibert et al., 2016), we observed the reverse at Station L1. This high affinity of nanophytoplankton for NH_4^+ at L1 would allow them to reduce energy costs and thus maintain high levels of production and productivity (Fig. 5) despite the presence of high-density

pearl cultures. Our results thus confirm that intense regeneration in areas with high pearl oyster densities favor high levels of production by nanophytoplankton (Lefebvre et al., 2012), which in return creates favorable conditions for pearl oyster growth.

The northwestern and eastern sites (Stations L10 and L8) are located in the northern circulation cell (Dumas et al., 2012). We found that those areas have different biogeochemical functioning compared to the SW part of the lagoon. Primary production at L10 and L8 was still mainly supported by regenerated production but the contribution of new production (based on NO_3^- uptake) was more important, representing 36 to 48 % of the total N uptake. There, organisms thus appear to be more adapted to the use of nitrate to meet their N needs. This may be explained by the existence of transient nitrate inputs such as the one recorded at stations L11 and L12 (Table 1) that might originate from internal upwelling generated by trade winds along the eastern side of the rim (Dumas et al., 2012; Fournier et al., 2012b; Fig. 2). The northern tip of the lagoon could receive additional nitrate inputs from bird guano due to its proximity to forested land with high bird densities, especially near the so-called “Bird Island” (just north of L11), and from enriched groundwater lenses. In addition, the water column in the northern cell is deeper and the lagoon broader which, combined with less pearl farming and fewer concessions per hectare (Supplementary Fig. S1), creates less favorable conditions for regeneration processes, despite long e-flushing times as in the SW part of the lagoon. The regenerated production at L8 and L10 was dominated by picoplankton and new production by larger organisms, which represent a classical pattern (Glibert et al., 2016).

Finally, the station near the pass (Station L4) exhibited the lowest C and N uptake rates and the lowest new production rates and f -ratios. The low uptake rates may be related to short e-flushing times in the central circulation cell due to tidal flushing through the pass and rapid water renewal (Dumas et al., 2012). The higher oceanic influence near the pass may also explain the low new production rates and f -ratios, considering that f -ratios in the surrounding oligotrophic ocean are also very low (< 0.1 , Raimbault et al., 2008), and assuming no upwelling occurred along the outer edge of the reef at the time of our study. Changes in the local plankton community, especially the presence of more oceanic organisms (Pagano et al., 2017; Thomas et al., 2010), may also impact C and N uptake in this area. Thus, the central cell in front near the pass appears to be different from the other cells in that its biological processes are highly influenced by lagoon-open ocean exchanges.

Together with these results, the observed spatial variations in nano-microphytoplankton assemblages could reflect changes in their trophic status as evidenced by N uptake data, especially given the taxon-specific differences in NH_4^+ and NO_3^- metabolism. Indeed, although the increased growth of diatoms coincided with an increase in new production due to the diatoms' preference of

oxidized rather than reduced substrates, they could not compete with the numerous flagellates in the SW who are better at exploiting the high concentrations of NH_4^+ or DON in that area (Glibert et al. 2016 and references therein). All these changes in phytoplankton community composition affect the energy and biomass transfer to higher trophic levels and can influence pearl oyster feeding and growth. Additional sampling with a greater space-time coverage would be necessary to complete this study and better understand the relationships between environment, phytoplankton taxa/species, and pearl oysters.

5. Conclusion

Results from this study yielded new insights into N cycling in Ahe lagoon through direct measurements of N uptake, obtained for the first time in this pearl farming atoll. The data highlighted the importance of regenerated production and showed that productivity in the lagoon relies primarily on fast internal nutrient recycling. In this context, the role of DON in nitrogen cycling and trophic pathways in the lagoon still needs to be investigated. By providing new C and N uptake data, this study also demonstrated the spatial heterogeneity of biogeochemical processes across the lagoon and confirms the link between the ecological functioning of the lagoon and its partitioning into hydrodynamically distinct water cells. The higher nutrient recycling capacity of the SW region associated with high primary and regenerated production appears to favor nanophytoplankton which directly benefits the growth of juvenile and adult oysters as well as spat collection (Thomas et al., 2012) and is likely a permanent feature. More generally, the spatial heterogeneity of trophic conditions, planktonic C and N fluxes, and species composition highlighted in this study may influence the transfer of energy through the food-web and have a direct impact on pearl oyster growth and reproduction including larval settlement potential, a hypothesis that could be tested using modelling approaches.

Due to our short sampling period, we could not capture the complete range of temporal variability of the relevant processes and more information is needed to extrapolate our findings to annual timescales. Nevertheless, it seems reasonable to state that the samples collected in this study should be representative of the warm, trade wind conditions that are typical for this region. It also seems plausible to assume that the observed dependence of primary production on regenerative processes is likely to persist throughout the year, as should the observed spatial differences in biogeochemical functioning. For primary production this has already been shown (Lefebvre et al., 2012). Presumably, the major sources of seasonal variability are linked to the intensity of processes modulated by changes in temperature and e-flushing times in the different parts of the lagoon which

affect the turnover of elements, something which could also be confirmed using numerical simulations.

The N and C uptake data presented here have already been included in a 0D modelling process to improve the configuration of a biogeochemical model that is currently being developed to simulate these particular atoll ecosystems. To examine the spatial heterogeneity of the biogeochemical processes, the model will be coupled to a 3D hydrodynamic model of this area. A realistic representation of biogeochemical cycles is essential to predict how changes in aquaculture will affect fluxes and stocks and vice versa, and the outcome of this work should be of great interest from a pearl farming management perspective.

Acknowledgements

This study was funded by the ANR-16-CE32-0004 MANA (Management of Atolls) project. The authors wish to thank Philippe Gérard (US IMAGO, New Caledonia) for providing nutrient data and Beatriz Beker for phytoplankton taxonomic identifications. We would also like to thank Patrick Raimbault for the chemical and isotopic analyses and fruitful discussions. Marc Pagano is acknowledged for his help with the statistical analyses and calculations of zooplankton grazing. We are also grateful to the “Direction des Ressources Marines” of French Polynesia for their logistics support and particularly to Gabriel Haumani for his help during field operations. Finally, we are grateful to two anonymous reviewers and to Serge Andréfouët for their advice and valuable comments which have greatly contributed to improve this manuscript.

References

- Aminot, A., Kérouel, R., 2007. Dosage automatique des nutriments dans les eaux marines: méthodes en flux continu. Editions Quae.
- Andréfouët, S., Pagès, J., Tartinville, B., 2001. Water renewal time for classification of atoll lagoons in the Tuamotu Archipelago (French Polynesia). *Coral Reefs* 20, 399–408.
- Andréfouët, S., Charpy, L., Lo-Yat, A., Lo, C., 2012. Recent research for pearl oyster aquaculture management in French Polynesia. *Marine Pollution Bulletin* 10(65), 407-414.
- Andréfouët, S., 2013. POLYPERL cruise, RV Alis, doi.org/10.17600/13100050.
- Andréfouët, S., Thomas, Y., Dumas, F., Lo, C., 2016. Revisiting wild stocks of black lip oyster *Pinctada margaritifera* in the Tuamotu Archipelago: the case of Ahe and Takaroa atolls and implications for the cultured pearl industry. *Estuarine, Coastal and Shelf Science* 182, 243-253.
- Andréfouët, S., Genthon, P., Pelletier, B., Le Gendre, R., Friot, C., Smith, R., Liao, V., 2020. The lagoon geomorphology of pearl farming atolls in the Central Pacific Ocean revisited using detailed bathymetry data. *Marine Pollution Bulletin* 160, 111580.
- Bouvy, M., Dupuy, C., Pagano, M., Barani, A., Charpy, L., 2012. Do human activities affect the picoplankton structure of the Ahe atoll lagoon (Tuamotu Archipelago, French Polynesia)? *Marine pollution bulletin* 65(10-12), 516-524.
- Bronk, D. A., See, J. H., Bradley, P., & Killberg, L., 2007. DON as a source of bioavailable nitrogen for phytoplankton. *Biogeosciences* 4, 283-296, doi.org/10.5194/bg-4-283-2007.
- Bythell, J. C., Wild, C., 2011. Biology and ecology of coral mucus release. *Journal of Experimental Marine Biology and Ecology* 408(1-2), 88-93.
- Charpy, L., Dufour, P., Garcia, N., 1997. Particulate organic matter in sixteen Tuamotu atoll lagoons (French Polynesia). *Marine Ecology Progress Series* 151, 55-65.
- Charpy-Roubaud, C.J., Charpy, L., Cremoux, J.L., 1990. Nutrient budget of the lagoonal waters in an open central South Pacific atoll (Tikehau, Tuamotu, French Polynesia). *Marine Biology* 107 (1), 67-73.
- Charpy-Roubaud, C., Charpy, L., Larkum, A., 2001. Atmospheric dinitrogen fixation by benthic communities of Tikehau Lagoon (Tuamotu Archipelago, French Polynesia) and its contribution to benthic primary production. *Marine Biology* 139(5), 991-998.
- Charpy, L., Rodier, M., Fournier, J., Langlade, M.J., 2012. Physical and chemical control of the phytoplankton of Ahe lagoon (French Polynesia). *Marine Pollution Bulletin* 65, 471-477.
- Dufour, P., Berland, B., 1999. Nutrient control of phytoplanktonic biomass in atoll lagoons and Pacific ocean waters: studies with factorial enrichment bioassays. *Journal of Experimental Marine Biology and Ecology*, 234(2), 147-166.
- Dufour, P., Andréfouët, S., Charpy, L., Garcia, N., 2001. Atoll morphometry controls lagoon nutrient regime. *Limnology and Oceanography* 46, 456-461.

- Dumas, F., Le Gendre, R., Thomas, Y., Andréfouët S., 2012. Tidal flushing and wind driven circulation of Ahe atoll lagoon (Tuamotu Archipelago, French Polynesia) from in situ observations and numerical modelling. *Marine Pollution Bulletin* 65(10-12), 425-440.
- Dupuy, C., Bouvy, M., Charpy, L., Fournier, J., Pagano, M., Durieux, B., et al., 2009. Planktonic compartment of Ahe Atoll (Tuamotu Archipelago, French Polynesia): potential preys for pearl oyster *Pinctada margaritifera*. 11th Pacific Science Inter-congress. Tahiti.
- Dutheil, C., Andréfouët, S., Jullien, S., Le Gendre, R., Aucan, J., Menkès, C., 2020. Characterization of south central Pacific Ocean wind regimes in present and future climate for pearl farming application. *Marine Pollution Bulletin* 160, 111584.
- Ferrier-Pagès, C., Leclercq, N., Jaubert, J., Pelegri, S.P., 2000. Enhancement of pico-and nanoplankton growth by coral exudates. *Aquatic Microbial Ecology* 21(2), 203-209.
- Ferrier-Pagès, C., Furla, P., 2001. Pico-and nanoplankton biomass and production in the two largest atoll lagoons of French Polynesia. *Marine Ecology Progress Series* 211, 63-76.
- Fournier, J., Dupuy, C., Bouvy, M., Couraudon-Réale, M., Charpy, L., Pouvreau, S., Le Moullac, G., Le Pennec, M., Cochard, J.C., 2012a. Pearl oysters *Pinctada margaritifera* grazing on natural plankton in Ahe atoll lagoon (Tuamotu archipelago, French Polynesia). *Marine Pollution bulletin* 65(10-12), 490-499.
- Fournier, J., Levesque, E., Pouvreau, S., Le Pennec, M., Le Moullac, G., 2012b. Influence of plankton concentration on gametogenesis and spawning of the black lip pearl oyster *Pinctada margaritifera* in Ahe atoll lagoon (Tuamotu archipelago, French polynesia). *Marine Pollution bulletin* 65(10-12), 463-470.
- Gueguen, Y., Gaertner-Mazouni, N., Lo, C., Le Moullac, G., 2016. Integrated management of pearl culture in French Polynesia in the context of global change: Synopsis of existing results. *Estuarine, Coastal and Shelf Science* 182, 229-234.
- Glibert, P. M., Wilkerson, F.P., Dugdale, R.C., Raven, J.A., Dupont, C.L., Leavitt, P.R., Kana, T.M., 2016. Pluses and minuses of ammonium and nitrate uptake and assimilation by phytoplankton and implications for productivity and community composition, with emphasis on nitrogen-enriched conditions. *Limnology and Oceanography* 61(1), 165-197.
- Goldman, J. C., Caron, D. A., & Dennett, M. R., 1987. Regulation of gross growth efficiency and ammonium regeneration in bacteria by substrate C: N ratio 1. *Limnology and Oceanography*, 32(6), 1239-1252.
- Harrison, W.G., Platt, T., Lewis, M. R., 1987. f-Ratio and its relationship to ambient nitrate concentration in coastal waters, *Journal of Plankton Research* 9 (1), 235–248, doi.org/10.1093/plankt/9.1.235.
- Hatcher, B.G., 1997. Coral reef ecosystems: how much greater is the whole than the sum of the parts? *Coral Reefs* 16, Suppl.:S77-S91
- Holmes, R. M., Aminot, A., Kérouel, R., Hooker, B. A., Peterson, B. J., 1999. A simple and precise method for measuring ammonium in marine and freshwater ecosystems. *Canadian Journal of Fisheries and Aquatic Sciences*, 56(10), 1801-1808.

- Ikeda, T. (1985). Metabolic rates of epipelagic marine zooplankton as a function of body mass and temperature. *Marine Biology*, 85(1), 1-11.
- Kieber, D. J., 2000. Photochemical production of biological substrates, in: *The effects of UV radiation in the marine environment*, edited by de Mora, S., Demers S., and Vernet, M., Cambridge University Press, Cambridge, pp. 131–148, 2000.
- Lacoste, É, Gueguen, Y., Le Moullac, G., Koua, M. S., Gaertner-Mazouni, N., 2014. Influence of farmed pearl oysters and associated biofouling communities on nutrient regeneration in lagoons of French Polynesia. *Aquaculture Environment Interactions* 5(3), 209-219.
- Lacoste, É, Gaertner-Mazouni, N., 2016. Nutrient regeneration in the water column and at the sediment–water interface in pearl oyster culture (*Pinctada margaritifera*) in a deep atoll lagoon (Ahe, French Polynesia). *Estuarine, Coastal and Shelf Science* 182, 304-30
- Le Bouteiller, A., Blanchot, J., & Rodier, M., 1992. Size distribution patterns of phytoplankton in the western Pacific: towards a generalization for the tropical open ocean. *Deep Sea Research Part A. Oceanographic Research Papers* 39(5), 805-823.
- Lefebvre, S., Claquin, P., Orvain, F., Véron, B., Charpy, L., 2012. Spatial and temporal dynamics of size-structured photosynthetic parameters (PAM) and primary production (^{13}C) of pico-and nano-phytoplankton in an atoll lagoon. *Marine pollution bulletin* 65(10-12), 478-489.
- Michotey, V., Guasco, S., Boeuf, D., Morezzi, N., Durieux, B., Charpy, L., Bonin, P., 2012. Spatio-temporal diversity of free-living and particle-attached prokaryotes in the tropical lagoon of Ahe atoll (Tuamotu Archipelago) and its surrounding oceanic waters. *Marine Pollution bulletin* 65(10-12), 525-537.
- Pagano, M., Sagarra, P. B., Champalbert, G., Bouvy, M., Dupuy, C., Thomas, Y., & Charpy, L., 2012. Metazooplankton communities in the Ahe atoll lagoon (Tuamotu Archipelago, French Polynesia): Spatiotemporal variations and trophic relationships. *Marine Pollution Bulletin*, 65(10-12), 538-548.
- Pagano, M., Rodier, M., Guillaumot, C., Thomas, Y., Henry, K., Andréfouët, S., 2017. Ocean-lagoon water and plankton exchanges in a semi-closed pearl farming atoll lagoon (Ahe, Tuamotu Archipelago, French Polynesia). *Estuarine, Coastal and Shelf Science* 191, 60-73, doi.org/10.1016/j.ecss.2017.04.017.
- Pouvreau, S., 1999. Study and modeling of mechanisms implied in growth of the black-lipped pearl oyster, *Pinctada margaritifera*, in the shellfish ecosystem of Takapoto lagoon, (French Polynesia). Pearl oyster physiology and growth model. Thesis. Ecole Nationale Supérieure d'Agronomie, Rennes (France).
- Pouvreau, S., Bacher, C., Héral, M., 2000. Ecophysiological model of growth and reproduction of the black pearl oyster, *Pinctada margaritifera*: potential applications for pearl farming in French Polynesia. *Aquaculture* 186(1-2), 117-144.
- Raimbault, P., Slawyk, G., Coste, B., Fry, J., 1990. Feasibility of using an automated colorimetric procedure for the determination of seawater nitrate in the 0 to 100nM range: Examples from field and culture. *Marine Biology* 104, 347–351, 1990.

- Raimbault, P., Pouvesle, W., Diaz F., Garcia, N., Sempéré, R., 1999. Wet-oxidation and automated colorimetry for simultaneous determination of organic carbon, nitrogen and phosphorus dissolved in seawater. *Marine Chemistry* 66, 161-169, 1999.
- Raimbault, P., Garcia, N., 2008. Evidence for efficient regenerated production and dinitrogen fixation in nitrogen-deficient waters of the South Pacific Ocean: impact on new and export production estimates. *Biogeosciences* 5, 323-338.
- Rix, L., De Goeij, J. M., Mueller, C. E., Struck, U., Middelburg, J. J., Van Duyl, F. C., Van Oevelen, D., 2016. Coral mucus fuels the sponge loop in warm-and cold-water coral reef ecosystems. *Scientific Reports*, 6(1), 1-11.
- Sakka, A., Legendre, L., Gosselin, M., LeBlanc, B., Delesalle, B., Price, N. M., 1999. Nitrate, phosphate, and iron limitation of the phytoplankton assemblage in the lagoon of Takapoto Atoll (Tuamotu Archipelago, French Polynesia). *Aquatic Microbial Ecology* 19(2), 149-161.
- Sangare, N., Lo-Yat, A., Le Moullac, G., Pecquerie, L., Thomas, Y., Lefebvre, S., le Gendre, R., Beliaeff, B., Andréfouët, S., 2020. Impact of environmental variability on *Pinctada margaritifera* life-history traits: A full life cycle deb modeling approach. *Ecological Modelling* 423, 109006.
- Torréton, J. P., Talbot, V., Garcia, N., 2000. Nutrient stimulation of bacterioplankton growth in Tuamotu atoll lagoons. *Aquatic Microbial Ecology*, 21(2), 125-137.
- Torréton, J. P., Pagès, J., Talbot, V., 2002. Relationships between bacterioplankton and phytoplankton biomass, production and turnover rate in Tuamotu atoll lagoons. *Aquatic Microbial Ecology* 28(3), 267-277.
- Tomas, C. R., 2016. *Identifying Marine Phytoplankton*. Academic Press, Inc. San Diego, California
- Thomas, Y., Garen, P., Courties, C., Charpy, L., 2010. Spatial and temporal variability of the pico-and nanophytoplankton and bacterioplankton in a deep Polynesian atoll lagoon. *Aquatic Microbial ecology* 59(1), 89-101.
- Thomas, Y., Garen, P., Pouvreau, S., 2011. Application of a bioenergetic growth model to larvae of the pearl oyster *Pinctada margaritifera* L. *Journal of Sea Research* 66(4), 331-339.
- Thomas, Y., Dumas, F., Andréfouët, S., 2014. Larval dispersal modeling of pearl oyster *Pinctada margaritifera* following realistic environmental and biological forcing in Ahe atoll lagoon. *PLoS One* 9(4), e95050.
- Thomas, Y., Dumas F., Andréfouët, S., 2016. Larval connectivity of pearl oyster through biophysical modelling: evidence of food limitation and broodstock effect. *Estuarine, Coastal and Shelf Science* 182, 283-293.
- Ward, B.A., Follows, M.J., 2016. Marine mixotrophy increases trophic transfer efficiency, mean organism size, and vertical carbon flux. *Proceedings of the National Academy of Sciences* 113(11), 2958-2963.
- WoRMS Editorial Board (2019) World Register of Marine Species. Available from the WoRMS web site : <http://www.marinespecies.org>.

Table 1. Mean nutrient, organic matter and Chla concentrations (total and % Chla >2 μm) in the Ahe lagoon between November 27 and December 7, 2017. The data represent the average (standard deviation) between depths of 3 and 20-30 m. Nutrients and organic matter are expressed in $\mu\text{mol L}^{-1}$, Chla in mg m^{-3} , and Chla >2 μm in % of total Chla.

Sites	NH_4^+	NO_x	PO_4^-	Si(OH)_4	DON	DOP	DOC	PON	POC	Chla_{tot}	% $\text{Chla}_{>2\ \mu\text{m}}$
L0	0.12 (0.01)	0.14 (0.08)	0.27 (0.01)	1.38 (0.12)				1.22 (0.05)	8.24 (1.96)	0.33 (0.02)	21 (3)
L1	0.06 (0.10)	0.21 (0.14)	0.28 (0.01)	1.66 (0.42)	10.1 (1.9)	0.40 (0.04)	85.6 (7.3)	1.93 (0.64)	17.77 (4.41)	0.38 (0.12)	21 (7)
L4	0.02 (0.01)	0.17 (0.05)	0.35 (0.02)	1.34 (0.17)	10.4 (2.9)	0.46 (0.03)	85.3 (16.6)	1.13 (0.08)	11.82 (1.67)	0.15 (0.03)	20 (2)
L8	0.01 (0.01)	0.12 (0.05)	0.33 (0.03)	1.33 (0.20)	12.2 (7.2)	0.51 (0.09)	78.7 (8.7)	1.06 (0.12)	10.18 (3.90)	0.13 (0.04)	17 (3)
L10	0.02 (0.02)	0.17 (0.05)	0.35 (0.01)	1.51 (0.23)	9.00 (1.4)	0.45 (0.02)	74.4 (5.8)	1.25 (0.26)	9.46 (2.48)	0.19 (0.04)	18 (3)
L11	0.04 (0.02)	0.33 (0.06)	0.36 (0.01)	1.20 (0.08)						0.13 (0.01)	19 (-)
L12	0.03 (0.02)	1.17 (0.74)	0.34 (0.02)	1.37 (0.02)						0.13 (0.05)	16 (1)

Table 2. Mean primary production (P) and ammonium and nitrate uptake rates (ρNH_4^+ , ρNO_3^-) in Ahe lagoon for the two size fractions $<2\ \mu\text{m}$ and $>2\ \mu\text{m}$. The data represent the depth-averages (between 3 and 20-30 m) with standard deviation given in parenthesis. Samples were performed in triplicate (duplicate at L0) during different days between November 27 and December 7, 2017.

Sites	L0	L1	L4	L8	L10
P $<2\ \mu\text{m}$ ($\text{mg C m}^{-3}\ \text{h}^{-1}$)	1.53 (0.14)	1.58 (0.47)	0.57 (0.21)	0.62 (0.24)	0.49 (0.11)
P $>2\ \mu\text{m}$ ($\text{mg C m}^{-3}\ \text{h}^{-1}$)	0.51 (0.09)	0.82 (0.36)	0.29 (0.16)	0.14 (0.10)	0.11 (0.13)
P/B _{Chla} $<2\ \mu\text{m}$ ($\text{mg C mg Chla}^{-1}\ \text{h}^{-1}$)	5.17 (1.14)	6.23 (1.83)	4.74 (1.63)	5.22 (1.33)	3.44 (0.97)
P/B _{Chla} $>2\ \mu\text{m}$ ($\text{mg C mg Chla}^{-1}\ \text{h}^{-1}$)	7.92 (0.90)	13.23 (5.21)	9.83 (2.84)	8.39 (3.48)	4.59 (2.38)
ρNH_4^+ $<2\ \mu\text{m}$ ($\mu\text{mol N m}^{-3}\ \text{h}^{-1}$)	29.51 (1.58)	15.58 (6.47)	5.27 (0.27)	9.59 (2.03)	7.56 (3.20)
ρNH_4^+ $>2\ \mu\text{m}$ ($\mu\text{mol N m}^{-3}\ \text{h}^{-1}$)	10.30 (2.44)	18.25 (5.58)	2.31 (2.06)	0.82 (1.08)	1.07 (1.49)
ρNO_3^- $<2\ \mu\text{m}$ ($\mu\text{mol N m}^{-3}\ \text{h}^{-1}$)	13.27 (4.49)	6.47 (5.23)	0.96 (0.04)	3.07 (0.67)	1.87 (1.22)
ρNO_3^- $>2\ \mu\text{m}$ ($\mu\text{mol N m}^{-3}\ \text{h}^{-1}$)	8.16 (4.74)	4.48 (3.52)	0.84 (0.74)	3.06 (2.38)	4.79 (2.79)
<i>f</i> -ratio (mol:mol)	0.34 (0.09)	0.23 (0.16)	0.20 (0.11)	0.36 (0.12)	0.49 (0.03)
<i>f</i> -ratio $>2\ \mu\text{m}$ (mol:mol)	0.42 (0.09)	0.18 (0.14)	0.34 (0.32)	0.83 (0.17)	0.94 (0.21)

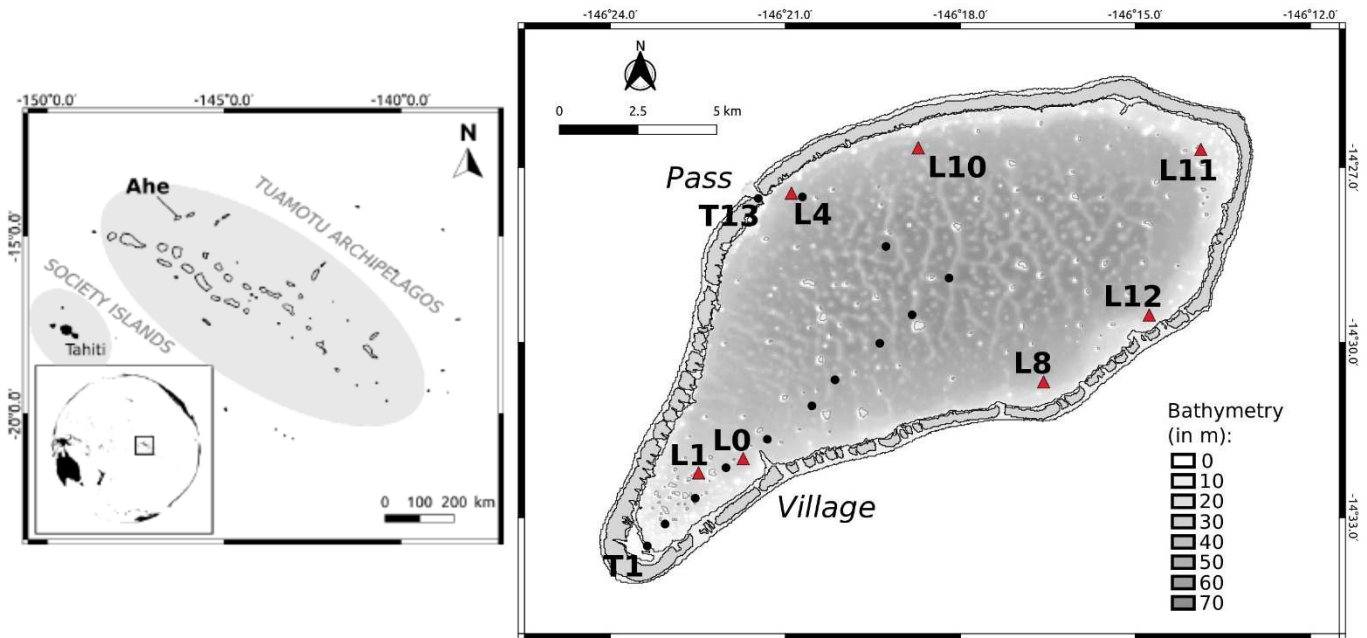


Figure 1. The Ahe atoll and the location of sampling stations. There are 7 fixed stations (“L” stations) where hydrology, phytoplankton abundance and rates were measured (red triangles) and 13 stations along a transect (black circles) where surface phytoplankton and CTD profiles were collected. The transect stations are consecutively numbered from T1 in the SW corner to T13 in the pass. See the supplementary material (Fig. S1) for the location of the oyster farms.

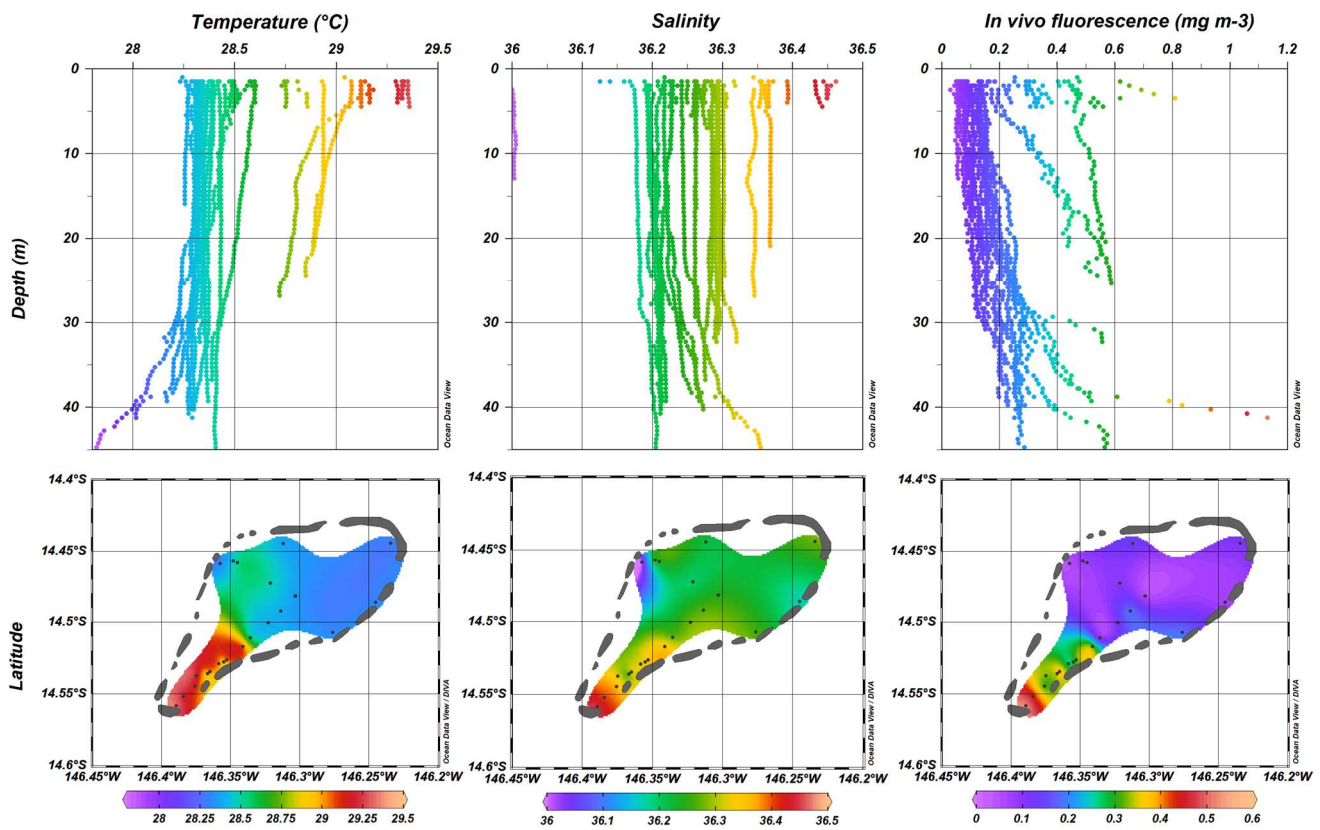


Figure 2. Vertical profiles (top panels) and 2D interpolations of the surface distribution (bottom panels) of temperature, salinity and *in vivo* fluorescence (used as a proxy of B_{Chla}) as obtained from Seabird profiling (39 profiles performed between 27 November and 7 December, 2017).

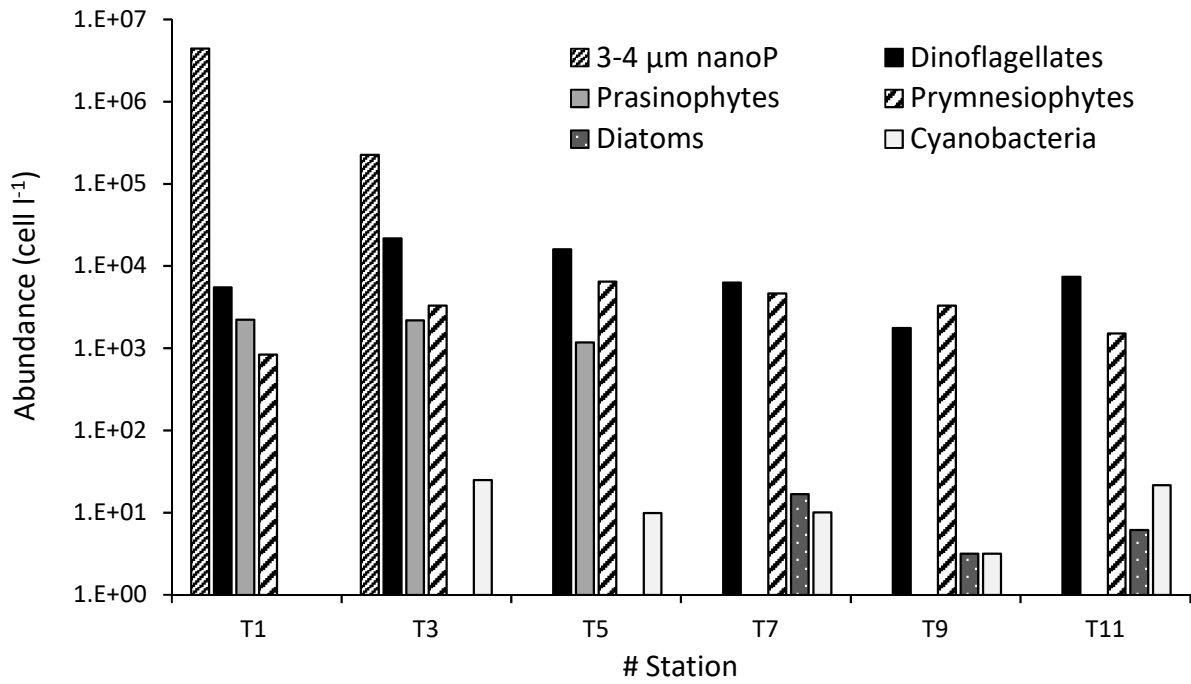


Figure 3. Abundance and taxonomic composition of nano-microphytoplankton at 3 m for different stations along the transect shown in Fig. 1 (from inverted microscopy data). 3-4 μm nanoP refers to unidentified nanophytoplankton. Cell abundance is presented on a logarithmic scale.

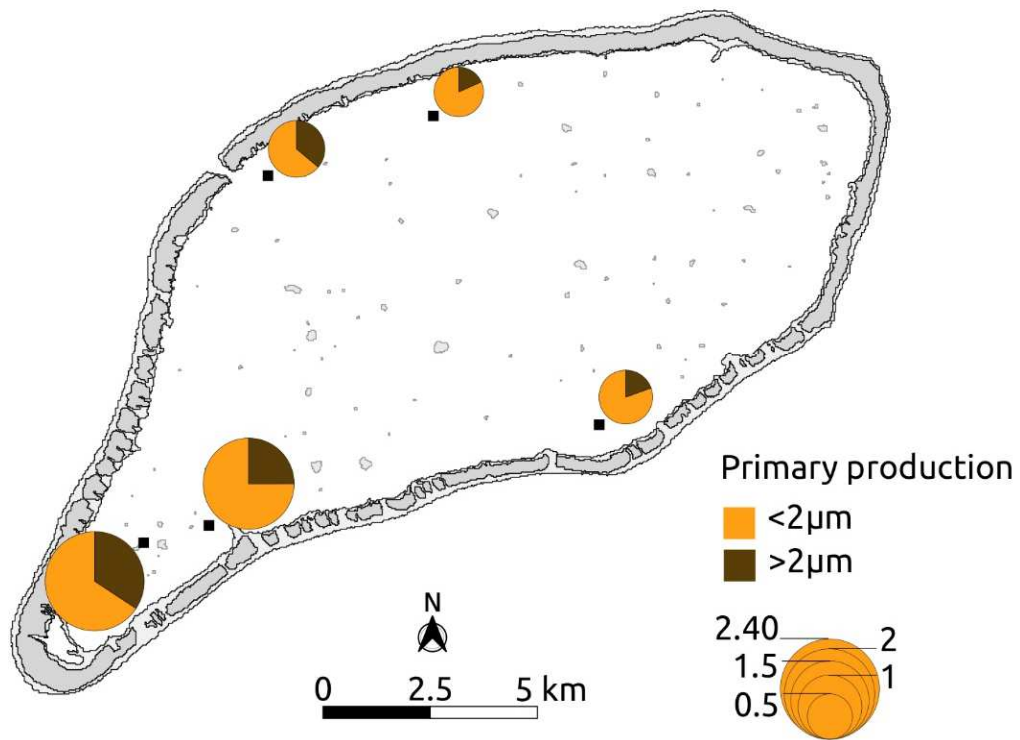


Figure 4. Mean primary production ($\text{mg C m}^{-3}\ \text{h}^{-1}$) in the Ahe lagoon for the two size fractions $<2\ \mu\text{m}$ and $>2\ \mu\text{m}$. Values represent the depth averages between 3 and 20-30 m (see Table 2).

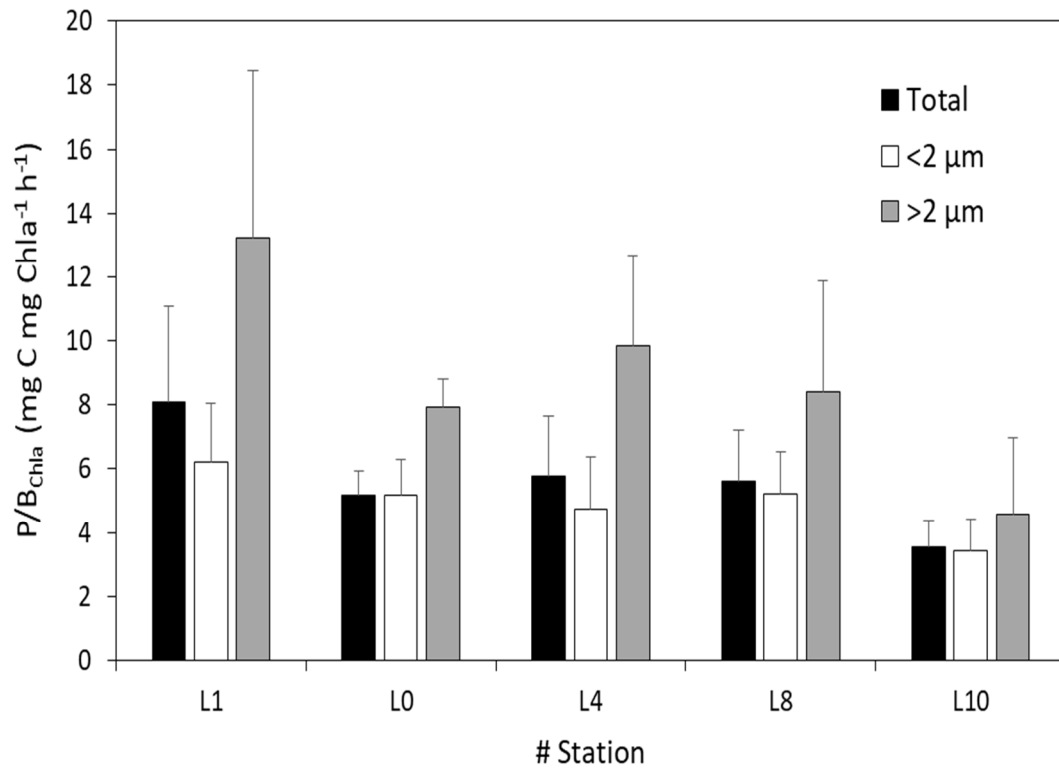


Figure 5. Total and size-fractionated biomass-specific primary production (P/B_{Chla}) in Ahe lagoon at the 5 stations sampled during November and December of 2017. Filler bars represent the depth-averaged values between 3 and 20-30 m with the error bars showing one standard deviation.

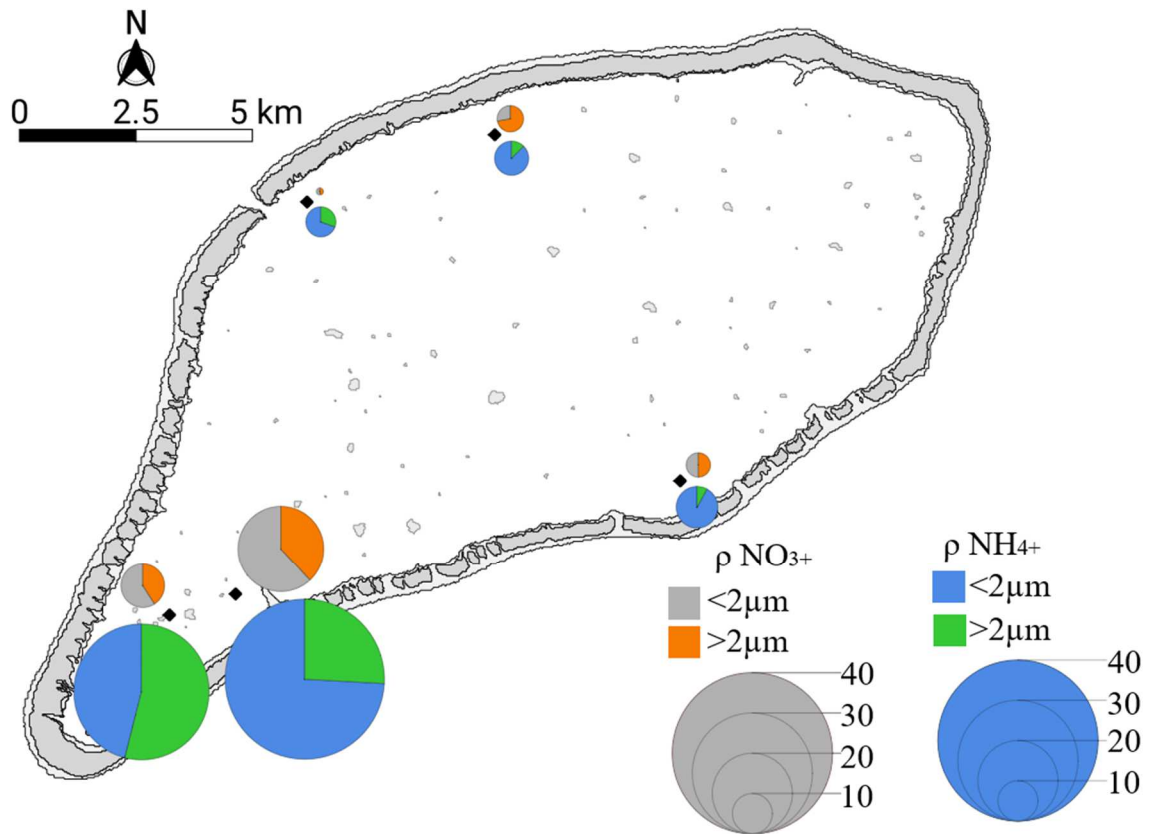


Figure 6. Mean NO_3^- and NH_4^+ uptake rates (ρNO_3^- , ρNH_4^+ , in $\mu\text{mol N m}^{-3} \text{ h}^{-1}$) for the two phytoplankton size fractions $<2\mu\text{m}$ and $>2\mu\text{m}$. Values were averaged between 3 and 20-30 m (see Table 2).